The defect structure with superabundant vacancies to be formed from fcc binary metal hydrides: Experiments and simulations

S. Harada, D. Ono, H. Sugimoto, Y. Fukai *

Department of Physics, Chuo University, Kasuga, Bunkyo-ku, Tokyo 112-8551, Japan

Abstract

The process of formation of defect hydrides containing a large number of metal-atom vacancies was studied experimentally in the fcc phase of Fe, Co, Ni and Pd, under different conditions of hydrogen pressure and temperature. Two distinctly different behaviors were observed: In metals with small formation energies of Vac–H clusters, both H and vacancies readily enter the metal lattice to attain the ultimate composition M_3VacH_4, whereas in metals with relatively large formation energies, the formation of this ultimate structure may become appreciable only at H concentrations exceeding some critical value. This general trend was confirmed by a model calculation including a long-range elastic interaction and short-range interatomic interactions between H atoms and vacancies.
© 2006 Elsevier B.V. All rights reserved.

1. Introduction

Since our discovery of superabundant vacancy (SAV) formation in Ni–H and Pd–H alloys in 1993 [1,2], this phenomenon has been studied rather extensively, and is now recognized as one of the fundamental properties of M–H alloys [3,4]. Sometimes, ordered defect structures containing a large number of SAVs become more stable than defect-free hydrides [2,5–10]. The basic mechanism of SAV formation is the lowering of the energy of interstitial H atoms neighboring vacancies, which in turn facilitates the formation of vacancies in the presence of interstitial H atoms. The formation energy of a Vac–H cluster (VacH$_r$) becomes $e_f^{cl} \approx e_f^v - re_b$, where e_f^v is the formation energy of a vacancy and e_b is the binding energy of an H atom to a vacancy. Up to now, values of the binding energy have been reported for a fairly large number of M–H systems [3,4,11,12], but the mechanism of how the formation of defect hydride structures depends on the binding energy, temperature and H concentration has not been clarified yet.

Here we address this problem by examining available experimental data, and performing model calculations on fcc-based M–H systems.

---

 * Corresponding author.
   E-mail address: yuh.fukai@m8.dion.ne.jp (Y. Fukai).

2. Experimental

Determination of the concentration of hydrogen (x_H) and Vac–H clusters (x_{cl}) has been made by XRD measurements of the temporal variation of the lattice parameter under high H pressures ($p_H \leq 6\,GPa$) and high temperatures ($T \leq 900\,°C$) [3,4,13]. The lattice parameter of a hydride sample decreases slowly over several hours from an initial value $a(0)$ to a final value $a(\infty)$ as Vac–H clusters are introduced.

The hydrogen concentration x_H can be estimated by comparing $a(0)$ with the lattice parameter of a metal without hydrogen a_0 under the corresponding p, T condition, *viz.*:

$$x_H = \frac{\Omega(0) - \Omega_0}{\Omega_H}, \tag{1}$$

where Ω_0 is the atomic volume ($\Omega_0 = a_0^3/4$), and Ω_H is the H-induced volume expansion.

On the other hand, the concentration x_{cl} may be estimated, approximately, from corresponding atomic volumes, $\Omega(0)$ and $\Omega(\infty)$, using a relation:

$$x_{cl} = \frac{\Omega(\infty) - \Omega(0)}{v_R^{cl}}, \tag{2}$$

where v_R^{cl} is the relaxation volume (lattice contraction) of a Vac–H cluster, defined in terms of the formation volume as $v_f^{cl} = \Omega_0 + v_R^{cl}$. In the absence of experimental values of v_R^{cl}, we may assume $v_R^{cl}/\Omega(0) = -0.36$, the average of calculated values for vacancies in a number of fcc metals [14]. The underlying assumption here is that in the course of vacancy formation the hydrogen concentration stays nearly unchanged, thus exerting no measurable effects on the lattice parameter. Validity of this assumption will be examined later.

In most of the experiments, samples were placed in the H_2 environment, and vacancy formation was observed in situ under a given high p_H, T condition. In
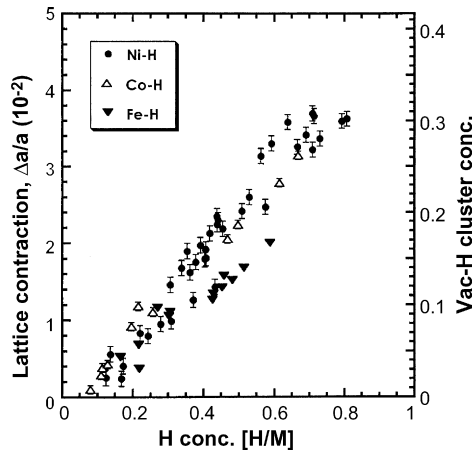
Fig. 1. Lattice contraction, the difference of lattice parameters of the initial and final state, $\Delta a = a(0) - a(\infty)$, of samples of Fe, Co, and Ni in contact with H_2 at high pressures and temperatures (open-system experiments) is plotted as a function of initial H concentration $x_H(0)$. Concentrations of Vac–H clusters, approximately estimated by $(3\Delta a/a)/0.36$, can be read from the right scale.

this method (an open-system method), the exchange of H with the environment in the course of vacancy formation is allowed. Results of such experiments on fcc Fe, Co and Ni are shown in Fig. 1 [13,15]. x_{cl} appears to be nearly proportional to x_H.

Results obtained for Pd are shown in Fig. 2, together with those on bcc Nb obtained earlier [13,16]. In these metals, where the solubility of hydrogen is large, samples were prepared in advance by electrolytic charging before being examined for vacancy formation. In this method (a closed-system method), the vacancy formation proceeds under a fixed H concentration. (Note, however, that the Pd data at high H concentrations ($x_H > 0.9$) were obtained by the open-system method.) In Pd, vacancy formation was monitored by XRD measurements as described above [13], and in Nb by resistance measurements [16]. The results indicate that the concentration of Vac–H clusters is more limited, and its dependence on H concentration is different from that of Fe, Co and Ni.
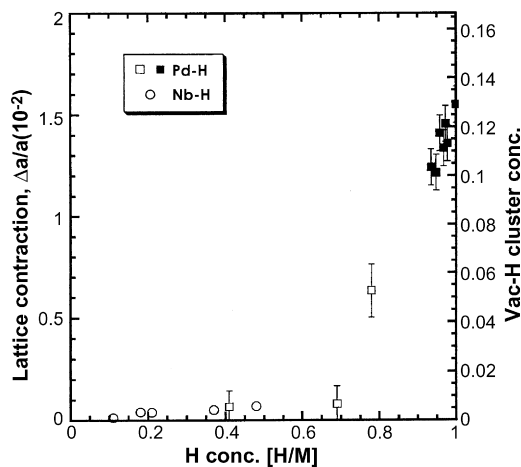

Fig. 2. Lattice contraction of Pd, the difference of lattice parameters of the initial and final state, $\Delta a = a(0) - a(\infty)$, is plotted as a function of initial H concentration $x_H(0)$. Open symbols from closed-system experiments and solid symbols from open-system experiments (see the text). Concentrations of Vac–H clusters in Pd, approximately estimated by $(3\Delta a/a)/0.36$, can be read from the right scale. For Nb, the cluster concentration has been obtained from resistivity measurements by the closed-system method.
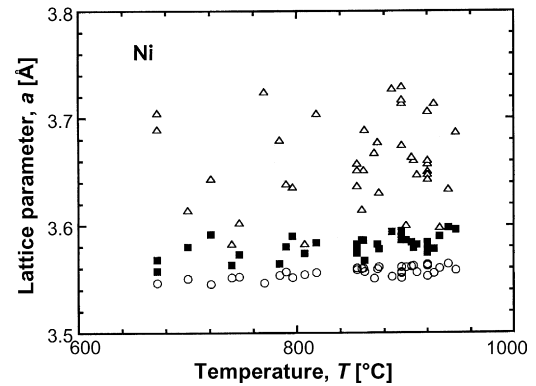

Fig. 3. Comparison of the lattice parameters of Ni obtained under different p_H, T conditions. The lattice parameters of the initial state $a(0)$ ($\triangle$), the final state $a(\infty)$ ($\blacksquare$) after hydrogenation, and that of the metal under the corresponding p, T condition a_0 ($\bigcirc$), are plotted as a function of temperature.

In order to identify the origin of these different behaviors, we examine the implication of the data obtained for Fe, Co and Ni, by re-plotting lattice parameters a_0, $a(0)$ and $a(\infty)$ measured at different p_H, Ts as a function of temperature. An example of such a plot for Ni is shown in Fig. 3. The lattice parameter of Ni (a_0) shows a small increase with temperature as a result of thermal expansion. (The scatter is due to the effect of pressure, which is different for each data point.) Significant to note is the fact that, although the lattice parameters immediately after hydrogenation ($a(0)$) differ widely depending on p_H, T conditions, the final lattice parameters ($a(\infty)$) resume very nearly the same value, slightly larger than a_0, with a thermal expansion similar to a_0. Very similar observations were made on Fe and Co. Thus, the apparent linear relation between x_H and x_{cl} for Fe, Co and Ni was simply the consequence of $a(\infty)$ being always close to a_0.

The implication of these results should be that, although initial H concentrations are different for different p_H, T conditions, after long holding times, samples in contact with surrounding H_2 attain the same ultimate structure. The ultimate structure is presumed to be the defect hydride of composition M_3VacH_4. The formation of a vacancy-ordered structure of this composition having a Cu_3Au-type metal lattice was observed in Pd–H [2], Mn–H [7] and Ni–H [8] systems, and its stability relative to a defect-free hydride structure of NaCl-type was confirmed by first-principles calculations [6,17,18]. (This vacancy-ordered structure is such that one of the four simple-cubic M-sublattices comprising the fcc structure becomes vacant, while leaving the H-sublattice intact.) A recent calculation by Zhang and Alavi [18] showed, moreover, that the lattice parameter of this ordered defect hydride is much smaller than the corresponding defect-free hydride, and comes close to that of the original metal. This is coherent with our observation that $a(\infty)$ is always slightly larger than a_0. In our XRD measurements quoted above, superlattice reflections were not observed, probably because of rather high temperatures, but the overall composition is believed to be close to this limit.

In most of the data shown in Fig. 2, where no such problems exist in the estimation of x_{cl}, we may accept the result at its face value, namely that the cluster concentration remains much lower in comparison to the case of Fe, Co and Ni.

We infer that this distinct difference in the behavior of the two groups of metals should be ascribed to the difference in the formation energy of a Vac–H cluster. Formation energies of a Vac–H cluster, estimated from known values of e_f^v and e_b for Fe, Co and Ni, are very small (-0.01 to 0.08 eV) [3,4], whereas those for Pd and Nb are much larger (0.72 eV for Pd [19] and 0.30 eV for Nb [16]).

Hence, the following picture emerges for the formation of defect hydrides. In metals where e_f^{cl} is small, both H and vacancies readily enter the metal lattice to attain the ultimate composition M_3VacH_4, whereas in metals where e_f^{cl} is relatively large, the formation of this ultimate structure may become appreciable only at H concentrations exceeding some critical value.

This general trend will be examined by Monte Carlo simulations in the next section.

3. Theoretical

The formation of a defect hydride structure is examined in the frame of a lattice-gas model, with a model Hamiltonian:

$$H = \tfrac{1}{2}\gamma B \Delta^2 V_0 + e_H n_H + e_v n_v + H_{int}, \tag{3}$$

where B is the bulk modulus, Δ the lattice dilatation, γ the image-force factor to include the free-surface effect [20,21], n_H and n_v the number of H atoms and vacancies, respectively, in volume V_0, and H_{int} represents the interaction between H atoms and vacancies. The elastic interaction is included in the energy of an H atom and a vacancy, in the form:

$$e_H = \mu_H - \alpha_H \Delta, \tag{4a}$$

$$e_v = \mu_v + \alpha_v \Delta, \tag{4b}$$

where α_H and α_v are taken to be positive.

In the lattice-gas model adopted here, n_H is written as a sum of occupation numbers of H atoms on interstitial sites n_i^H, viz. $n_H = \sum_i n_i^H$, where n_i^H assumes either 1 or 0 for occupied or unoccupied site i. Similarly, $n_v = \sum_l n_l^v$, with n_l^v either 1 or 0 for M-atom site l occupied or unoccupied by a vacancy, respectively. The interaction term is formally written as

$$H_{int} = \frac{1}{2}\sum_{i,j} J_{ij}^H n_i^H n_j^H + \frac{1}{2}\sum_{l,m} J_{lm}^v n_l^v n_m^v + \sum_{i,l} V_{il} n_i^H n_l^v, \tag{5}$$

with the three terms representing, in order, the H–H, Vac–Vac and H–Vac interactions, for which the following simplifying assumptions are made:

(1) No two H atoms can occupy the same interstitial site, and no direct interaction operates between any two H atoms.
(2) No two vacancies can occupy nearest M-atom sites.
(3) The interaction operates between a vacancy and an H atom on any nearest interstitial site. The interaction between the Vac–H pair is assumed to be attractive, with the interaction energy $-e_b$ ($e_b > 0$).

The partition function of the system is

$$Z = \int_{-\infty}^{\infty} d\Delta \sum_{\{H\}} \sum_{\{v\}} \exp\left(-\frac{H}{kT}\right) = \sqrt{\frac{2\pi}{\gamma B V_0}} Z_1, \tag{6}$$

$$Z_1 = \sum_{\{H\}} \sum_{\{v\}} \exp\left(-\frac{H_1}{kT}\right), \tag{7}$$

where

$$H_1 = \mu_H n_H + \mu_v n_v - \frac{\alpha_H^2}{2\gamma B V_0}\left(n_H - \frac{\alpha_v}{\alpha_H} n_v\right)^2 + H_{int}. \tag{8}$$

Using this, thermal average quantities can be calculated

$$\langle n_H \rangle = \frac{1}{Z_1} \sum_{\{H\}} \sum_{\{v\}} n_H \exp\left(-\frac{H_1}{kT}\right), \tag{9}$$

$$\langle n_v \rangle = \frac{1}{Z_1} \sum_{\{H\}} \sum_{\{v\}} n_v \exp\left(-\frac{H_1}{kT}\right), \tag{10}$$

and

$$\langle \Delta \rangle = \frac{\alpha_H \langle n_H \rangle - \alpha_v \langle n_v \rangle}{\gamma B V_0}. \tag{11}$$

In the absence of vacancies, we have $\alpha_H = \gamma B \langle \Delta \rangle V_0 / \langle n_H \rangle = \gamma B \Omega_H$, and similarly $\alpha_v = -\gamma B v_R^v$, which we write $\alpha_v = \gamma B \Omega_v$ by using the positive quantity $\Omega_v = -v_R^v$.

Calculations were performed by Monte Carlo method, allowing for introduction/removal of H atoms and vacancies. The system consists of an fcc metal lattice of $N_0 = 4000$ sites and an H sublattice of an equal number of octahedral interstitial sites, repeated by periodic boundary conditions. The parameters adopted are appropriate for Ni: $\mu_v = 1.8$ eV [22], $\gamma = 0.4$ [21], $B = 190$ GPa, $\Omega_0 = 10.9$ Å^3 and $\Omega_H = 2.2$ Å^3 [23], which gives $\alpha_H^2/\gamma B \Omega_0 = \gamma B \Omega_H^2/\Omega_0 = 0.2$ eV. For the parameter α_v/α_H, we assume a value 3.0, which is a little larger than $\Omega_v/\Omega_H = 0.36 \times 10.9/2.2 = 1.8$. The reason for this choice will be described later.

Hereafter, the concentrations of H and vacancies are expressed as per site, i.e. $x_H = \langle n_H \rangle/N_0$ and $x_v = \langle n_v \rangle/N_0$. They correspond, respectively, to x_H and x_{cl} used in the preceding section.

In order to facilitate comparison with the experimental results shown in Figs. 1 and 2, the lattice contraction caused by the introduction of vacancies and H atoms was calculated as $\Omega(0) - \Omega(\infty) = \Omega_v x_v(\infty) - \Omega_H(x_H(\infty) - x_H(0))$, and the results are shown in Fig. 4, as a function of initial H concentration $x_H(0)$. The calculation was performed at a fixed temperature $kT = 0.1$ eV ($T = 1160$ K), for five different values of the binding energy e_b.

The overall dependence changes abruptly at a certain value of e_b. For $e_b > 0.40$ eV, the volume contraction increases nearly
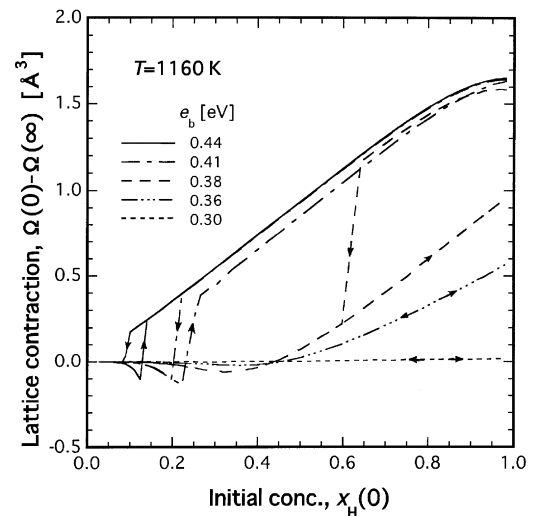

Fig. 4. The volume contraction $\Omega(0) - \Omega(\infty)$ calculated by Monte Carlo simulations as a function of initial H concentration $x_H(0)$. Calculations have been performed at a fixed temperature ($T = 1160$ K), for five different values of the Vac–H binding energy e_b. Note the appearance of hysteresis for relatively large values of e_b.
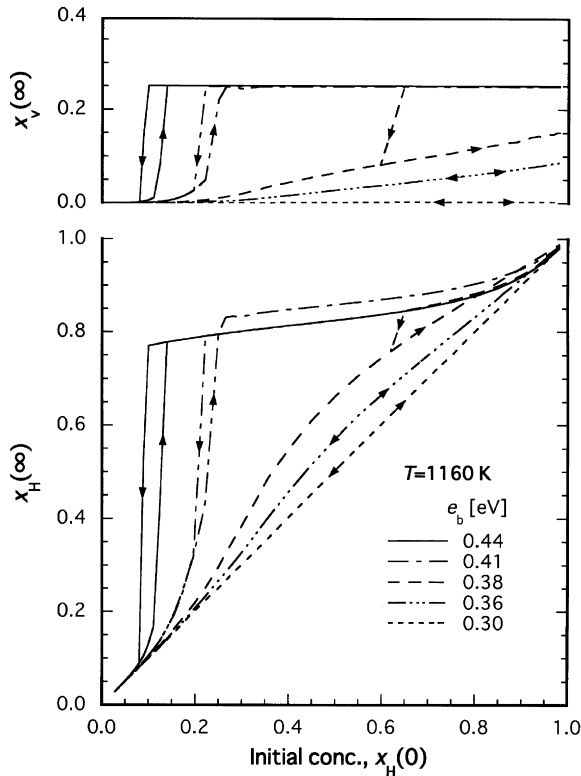
Fig. 5. Final concentrations of H atoms (bottom figure) and vacancies (top figure), $x_H(\infty)$ and $x_v(\infty)$, respectively, that underlie the volume contraction shown in Fig. 4. Calculations have been performed at a fixed temperature ($T = 1160$ K), for five different values of the Vac–H binding energy e_b. Note a strong tendency for the formation of M_3VacH_4 for large values of e_b.

proportionally to $x_H(0)$, whereas for $e_b < 0.36$ eV, it stays rather small over a wide range of $x_H(0)$.

The concentrations of H atoms and vacancies in the final state that have caused this volume change, $x_H(\infty)$ and $x_v(\infty)$, are shown in Fig. 5, as a function of $x_H(0)$. For the strong binding ($e_b > 0.40$ eV), the composition quickly changes to $M_3VacH_{\sim 3}$ ($x_H(\infty) \sim 0.8$ and $x_v(\infty) = 0.25$) for any initial H concentrations. For the weaker binding ($e_b < 0.36$ eV), on the other hand, smaller amounts of H and vacancies are introduced. Significant to note is the appearance of hysteresis for the intermediate values of e_b.

For evaluating the implication of these results, it is necessary to elucidate the actual calculation procedure how a series of data points were obtained in increasing and decreasing initial H concentrations. The procedure is as follows:

(1) Start with a vacancy-ordered hydride M_3VacH_4 (Cu_3Au-type metal lattice), with $x_H(0) = 1$ and $x_v(0) = 0.25$, corresponding to sufficiently low values of μ_H.
(2) Increase μ_H by an appropriate amount to remove a small amount of H.
(3) Allow introduction/removal of H atoms and vacancies repeatedly until new equilibrium is attained. Calculate the concentrations of H atoms and vacancies by taking the average over 2,400,000 subsequent repetitions (300 repetitions per site for both H atoms and vacancies) in this equilibrium state.

(4) Repeat (2) and (3) until sufficiently low H concentration is reached.
(5) Decrease μ_H by an appropriate amount to induce a small increase of H.
(6) Allow introduction/removal of H atoms and vacancies until new equilibrium is attained. Calculate the average concentrations of H atoms and vacancies as in (3).
(7) Repeat (5) and (6) until sufficiently high H concentration is reached.

The appearance of hysteresis indicates that there is an energy barrier between the two states, a vacancy-rich state and a vacancy-poor state, and sufficiently high thermal energies are required to surmount this barrier. Indeed, at higher temperatures jumps to the vacancy-rich state occur at lower H concentrations.

4. Discussion

It is shown in the foregoing sections that for strong Vac–H binding (corresponding to small e_f^{cl}) the ultimate defect hydride M_3VacH_{3-4} readily forms, whereas for weak binding (corresponding to large e_f^{cl}) only a limited introduction of Vac–H clusters may take place. The former corresponds to the case of Fe, Co and Ni, and the latter to Pd and Nb. In this connection, it may be noted in Fig. 5(bottom) that, for small Vac–H binding energies, the introduction of hydrogen in the course of vacancy formation (deviation from the 45° line) is consistently small, which implies in effect that the distinction between the open- and closed-system conditions should be rather unimportant. This justifies the comparison of the present calculation with the observation in Pd and Nb by closed-system experiments. It may be added here that this argument is also supported by preliminary calculations assuming fixed H concentrations in the vacancy formation process.

For more detailed comparison with the experiments, possible limitations of the model calculation have to be examined. Of the two parameters describing the elastic interaction, the parameter $\gamma B \Omega_H^2 / \Omega_0 = 0.2$ eV, calculated from known materials parameters of Ni, was found to reproduce the spinodal decomposition temperature of the Ni–H system $kT_c = 0.5$ eV ($T_c = 580$ K) [24,25], which gives endorsement to this choice of the parameter. On the other hand, the ratio $\alpha_v/\alpha_H = 3.0$ has been chosen, *ad hoc*, to bring the lattice parameter of M_3VacH_4 into agreement with experiments. A choice of $\alpha_v/\alpha_H = \Omega_v/\Omega_H = 1.8$, legitimate for isolated H atoms and vacancies, has led to larger volume expansion for defect hydrides, a result less consistent with the observation. This implies that lattice contraction around a vacancy with trapped H atoms should be larger than that of an isolated vacancy. In fact, evidence in support of this has been provided by the results of our high p, T experiments that reduction of the equilibrium cluster concentration due to a pv term in the formation enthalpy is rather limited even at pressures of several GPa. Under those conditions, isolated vacancies in metals with the formation volume $v_f^v \sim (1 - 0.36)\Omega_0$ ranging between 7 and 10 Å^3, hence $pv_f^v = 0.2$–0.3 eV for $p = 5$ GPa, should have been subject to appreciable reductions of the equi-

librium concentration. Thus, for Vac–H clusters, the formation volume $v_f^{cl} = \Omega_0 + v_R^{cl}$ should be smaller due to larger magnitudes of the volume relaxation $|v_R^{cl}|$.

5. Summary

The formation of defect structure with superabundant M-atom vacancies has been studied on fcc-based M–H alloys. Two distinctly different formation processes have been observed, and explained, both experimentally and theoretically, in terms of different formation energies of Vac–H clusters.

References

[1] Y. Fukai, N. Ōkuma, Jpn. J. Appl. Phys. 32 (1993) L1256.
[2] Y. Fukai, N. Ōkuma, Phys. Rev. Lett. 73 (1994) 1640.
[3] Y. Fukai, J. Alloys Compd. 356/357 (2003) 263.
[4] Y. Fukai, The Metal–Hydrogen System, 2nd ed., Springer, 2005 (Sect. 5.6).
[5] D.S. dos Santos, S. Miraglia, D. Fruchart, J. Alloys Compd. 291 (1999) L1.
[6] S. Miraglia, D. Fruchart, E.K. Hlil, S.S.M. Tavares, D. dos Santos, J. Alloys Compd. 317 (2001) 77.
[7] Y. Fukai, T. Haraguchi, E. Hayashi, Y. Ishii, Y. Kurokawa, J. Yanagawa, Defect Diffusion Forum 194–199 (2001) 1063.
[8] Y. Fukai, Y. Shizuku, K. Kurokawa, J. Alloys. Compd. 329 (2001) 195.
[9] D. Kyoi, T. Sato, E. Rönnebro, Y. Tsuji, N. Kitamura, A. Ueda, M. Ito, S. Katsuyama, S. Hara, D. Noréus, T. Sakai, J. Alloys Compd. 375 (2004) 253.
[10] T. Sato, D. Kyoi, E. Rönnebro, N. Kitamura, T. Sakai, D. Noréus, J. Alloys Compd. 417 (2006) 230.
[11] W. Möller, F. Besenbacher, J. Bøttiger, Appl. Phys. A27 (1982) 19.
[12] S.M. Myers, P.M. Richards, W.R. Wampler, F. Besenbacher, J. Nucl. Mater. 165 (1989) 9.
[13] S. Harada, S. Yokota, T. Ishii, Y. Shizuku, M. Kanazawa, Y. Fukai, J. Alloys Compd. 404–406 (2005) 247.
[14] P.A. Korzhavyi, I.A. Abrikosov, B. Johansson, A.V. Ruban, H.L. Skriver, Phys. Rev. B 59 (1999) 11693.
[15] T. Hiroi, Y. Fukai, K. Mori, J. Alloys. Compd. 404–406 (2005) 252.
[16] H. Koike, Y. Shizuku, A. Yazaki, Y. Fukai, J. Phys.: Condens. Matter 16 (2004) 1335.
[17] E.K. Hlil, D. Fruchart, S. Miraglia, J. Tabola, J. Alloys Compd. 356/357 (2003) 169.
[18] C. Zhang, A. Alavi, J. Am. Chem. Soc. 127 (2005) 9808.
[19] Y. Fukai, Y. Ishii, T. Goto, K. Watanabe, J. Alloys Compd. 313 (2000) 121.
[20] J.D. Eshelby, in: F. Seitz, D. Turnbull (Eds.), Solid State Physics, vol. 2, Academic Press, 1956, p. 79.
[21] Y. Fukai, The Metal–Hydrogen System, 2nd ed., Springer, 2005 (Sect. 2.2).
[22] P. Ehrhart, P. Jung, H. Schultz, H. Ullmaier, in: H. Ullmaier (Ed.), Atomic Defects in Metals, Landolt-Börnstein New Series, vol. 25, Springer, 1993.
[23] Y. Fukai, The Metal–Hydrogen System, 2nd ed., Springer, 2005 (Sect. 4.2).
[24] Y. Fukai, S. Yamamoto, S. Harada, M. Kanazawa, J. Alloys Compd. 372 (2004) L4.
[25] Y. Fukai, J. Alloys Compd. 404–406 (2005) 7.